The significance of the properties of water for the working cycle of the kinesin molecular motor

Anna Kuffel, and Monika Szałachowska

Citation: The Journal of Chemical Physics **148**, 235101 (2018); doi: 10.1063/1.5020208
View online: https://doi.org/10.1063/1.5020208
View Table of Contents: http://aip.scitation.org/toc/jcp/148/23
Published by the American Institute of Physics

The significance of the properties of water for the working cycle of the kinesin molecular motor

Anna Kuffel[a] and Monika Szałachowska
Faculty of Chemistry, Department of Physical Chemistry, Gdansk University of Technology, Narutowicza 11/12, 80-233 Gdansk, Poland

(Received 21 December 2017; accepted 25 May 2018; published online 19 June 2018)

Explicit solvent molecular dynamics simulations were performed in this study to investigate and discuss several aspects of the influence of the properties of water on the working cycle of a molecular motor from the kinesin superfamily. The main objects of attention were: the binding of the neck linker and the association of the kinesin and the tubulin. The docking of the neck linker is considered a crucial event during the working cycle and is said to be the one that contributes to propelling the motor forward. Herein, it is demonstrated that the solvent contributes to the force-generating mechanism of the motor—the absolute value of the force generated by the linker depends on the properties of the solvent. The force can also depend on the instantaneous conformation of the protein. Our results show that the force may not be strictly the same during every step, as well as during the whole process of the docking, but we checked that even the smaller forces measured by us were big enough to propel the kinesin head along the protofilament with the required speed. It is also shown that the dynamics of the process of approach of the kinesin to its binding site on the microtubule track changes rapidly as the proteins come closer. The influence of the properties of interfacial water on the kinetics of this process is discussed here. *Published by AIP Publishing.* https://doi.org/10.1063/1.5020208

I. INTRODUCTION

Molecular motors belonging to the kinesin superfamily are able to move across the cell along tracks formed by microtubules. The working cycle of a conventional kinesin consists of several phases that are relatively well described, although the details are still under debate.[1] In the case of a two-headed kinesin, the main phases of a single step include the following:[2] dissociation of the trailing head from the surface of the microtubule, the forward movement of the head through the solvent, and the attachment of the head to the microtubule in the next binding site. The motor is fueled by the hydrolysis of adenosine triphosphate (ATP).

While discussing the work of the motor, much attention is usually put to the mechanical properties of the proteins (such as the conformational changes and the strain in the elongated polypetide chains)[3] but also to the electric field generated by the microtubule and the kinesin, thanks to their nonzero net charges.[4,5] From this perspective, solvent is no more than a passive environment. However, it is known that the properties of the solvent can influence the behavior of the proteins in many complex ways.[6–14] Because of this, herein, a slightly different approach is taken and the concentration is on the possible influence of the properties of the solvent on the selected phases of the working cycle of the motor, specifically on the docking of the neck linker and on the approach of the kinesin head to the binding site on the microtubule. Accordingly, the three main goals of the article are to discuss: (1) whether the properties of water can influence the values of the force generated by the motor upon the neck linker docking, (2) whether the measured force suffices to effectively pull the kinesin head along the microtubule, and (3) how the process of the association of the kinesin head and the tubulin dimer can be influenced by the properties of water. The discussion on how the work of the motor is shaped by the solvent is the common core of all these three goals. This subject is relevant not only to kinesins but also to proteins in general. We used molecular dynamics, all-atom models, and explicit solvent. As it is known, this method offers greater reliability and produces more realistic results than coarse-grained models and/or implicit solvent simulations[15] that have been routinely used in studies of the kinesin dynamics performed to this date. Several recent attempts to simulate the movement of the kinesin along the microtubule are described in Refs. 4, 5, 16, and 17. All of these simulations used heavily simplified models. Currently, it is impossible to simulate a whole step of the kinesin using an all-atom model and explicit solvent.

During the working cycle of the kinesin, the neck linker alternately binds to the catalytic domain and unbinds from it.[18,19] The docking very early became a candidate for the structural change that greatly contributes to propelling the motor forward.[20] Since then, its significance for the movement has been extensively debated.[18,21] The hypothesis that the neck linker might be involved in the power stroke that moves the motor forward has been questioned because of the flexibility and relatively small size of the linker[21] and because of the moderate strength of interactions with the catalytic domain.[21,22]

As it has been demonstrated by Hwang *et al.*[23] by computer simulations, the neck linker on its own is indeed unable

[a]anna.kuffel@pg.edu.pl

to generate any relevant force. However, the neck linker can bind with several N-terminal amino acids, called a cover strand (CS), to form a structure called "cover neck bundle" (CNB).[23] The junction with the cover strand can result in an increased stiffness of the neck linker and cause a greater conformational bias to the binding site. As a result, the force exerted by the cover neck bundle may be significant. Hwang *et al.*[23] used for their measurements a small fragment of the kinesin motor domain (almost only an isolated CNB). They observed that the vectors of the force exerted by a bent CNB pointed directly in the direction of the docking site—even though the docking site itself was not present in the investigated part of the protein.

Also, Hesse *et al.*[24] calculated forces for isolated CNBs of kinesin-1 and kinesin-5 in implicit solvent. They obtained qualitatively comparable results and found that forces generated by the CNB of kinesin-5 are a bit lower.

However, it is not ubiquitous for all kinesins that the vectors of the force point to the direction of the expected movement. Lakkaraju and Hwang[25] measured forces exerted by the neck of a minus-end-directed kinesin Ncd. The directions of the vectors were not related to the trajectory of that structural element. Because of this, the authors suspected that the conformational change is diffusion-dependent and guided by the sequential creation of intermediate contacts with the head.

The differences between these results might be explained not only by the different mechanisms of structural rearrangements but also by the fact that the methodology of both these measurements was different. The investigations described in Ref. 23 were performed with only a small fragment of the motor domain (amino acids 1-12 and 317-331). This structure was partially restrained to keep it in place during the measurements (carbon alpha atoms of amino acids 9-12 and 317-323 were fixed in space to anchor the base of the CNB, and harmonic constraints on the backbone hydrogen bonds were applied to prevent them from breaking). When the linker, stiffened by the presence of the CNB, was bent from its natural conformation, the clear conformational bias was detected. However, that study did not take into account, for example, the presence of the docking site on the surface of the kinesin head. Also, the whole fragment was significantly more restrained than it is in the natural conditions. It is flexibly attached to the rest of the protein and not to a short, restrained helix.

Because in the study described in Ref. 25 the whole kinesin head was used, the overall flexibility of the investigated mechanical system and the available conformational space were greatly increased relatively to Ref. 23. In these conditions, there was no clear relationship between the vectors of the force and the trajectory.

In face of these divergent literature data, we decided to investigate a more complex and more realistic model of the kinesin than in Ref. 23 (a whole motor domain) to examine whether we obtain a picture closer to the one described in Ref. 23 or closer to the case of Ncd, described in Ref. 25.

Moreover, Hwang *et al.*[23] observed that the value of the force generated by the CNB could be different (though qualitatively comparable) when explicit and implicit solvents were used for the simulation. They did not elaborate on this difference. In our opinion, this result emphasizes the importance of solvation. It also might suggest that the influence of the changes in the properties of the solvent on the force should be observed.

The role of water in the docking was noticed by Yan-Bin *et al.*[26] They suggested that water molecules can assist the process by forming hydrogen-bonded water bridges at those positions where direct hydrogen bonding is hindered. Moreover, the hydrogen bond network can also stabilize the contacts made due to the hydrophobic interactions. These were other reasons why we believed that the properties of the solvent might influence the work of the motor. Therefore, we compared the forces generated by the protein immersed in one of commonly used water models and two slightly modified water models. This is described in detail in the Methods section. It allowed us to grasp the influence of the properties of the solvent on the generation of the force. We discovered that the measured values of the force were different for solvents with varying properties, what implies that water participates in the force-generating mechanism—a factor that has been so far overlooked when discussing the work of the motor.

If the force that the neck linker is able to generate is big enough to propel the kinesin forward along a microtubule protofilament in time corresponding to the measured velocity of the stepping of the kinesin, then we can assume that this structural element is in fact involved in the power stroke. To check this, we also constructed systems consisting of a kinesin head and a five-tubulin-long protofilament. Then, the force of several different magnitudes (comparable with the ones measured for the CNB) was applied to the neck helix of the kinesin and the displacement of the kinesin head was measured.

The second process that was analyzed by us was the association of the kinesin and the tubulin. It is generally acknowledged that the solvent can passively and actively participate in the association and dissociation of proteins.[6–8] The behavior of the solvent during these processes can be very case-specific and subject to changes in the geometry and chemical character of the interacting surfaces.[9] The association of proteins is often connected with major or minor structural changes in proteins themselves, and these changes can also be influenced by the solvent (since the properties of the solvent can influence the conformation and inner motions of macromolecules[10–14]).

It is a prevailing view that to make a forward step, the motor needs to make a diffusional excursion in the right direction.[16,27] The diffusion rate of a solute, of course, depends strongly on the properties of the solvent. In relation to kinesin, the importance of the effects present due to hydration was recently demonstrated by Goldtzvik *et al.*[17] They created a coarse-grained model of the complex of kinesin with microtubule and observed that it is crucial to include hydrodynamic interactions[28] in simulations to obtain quantitative agreement with experiments when it comes to the time needed to complete a single step. The inclusion of hydrodynamic interactions speeds up diffusion of the detached head and thus enables it to reach its target binding site much faster.

Previously,[29,30] we described how some properties of water are changed in the region between the kinesin head and the tubulin dimer. These changes include slowed down diffusional motion, the blue shift of the spectra of the translational velocity autocorrelation function (explained by increased stiffness of interfacial water), increased density, the distortion of the geometry of the hydrogen bond network, and partial ordering of water molecules by the electric field generated by the proteins. The changes in properties of water between proteins can be more profound than in the case of a single protein.

As we observed,[30] the changes in the dynamical features of solvation water of the kinesin head that take place under the influence of the presence of the tubulin dimer lead to the changes in the pattern of the internal vibrations of the kinesin head. The impact was best visible for the low-frequency range, up to about 2 THz. It is the range that is especially important for the biological function of proteins.[31] As we also found out, the collective movements of surface atoms of kinesin and tubulin can become correlated to some extent (although the effect is relatively weak).[32] We suggested that the network of hydrogen bonds spanning from one protein surface to the other may be involved in this process. This supposition was supported by our results obtained with the use of modified water models.[32] The use of water model that, on average, created more hydrogen bonds led to the higher cross-correlation coefficients. This emphasizes the role of properties of water in the intermolecular interactions.

The changes in the structure and dynamics of solvation water between the kinesin and the tubulin can influence not only their internal motions but it might be expected that their relative movement (the process of the association and hence the dynamics of the stepping) could also be affected.

II. METHODS

Our three goals, all related to the significance of the solvent for the working cycle of the kinesin molecular motor, were: (1) to measure the force in different solvents to prove that the solvent participates in the force-generating mechanism (and to check the dependence on the conformation of the protein), (2) to drag the kinesin head along the short protofilament to investigate what force would be needed to effectively propel the head forward, and (3) to investigate the association of the kinesin and the tubulin dimer and discuss some properties of the solvent that may influence the kinetics of this process. To achieve them, we had to construct three different types of systems and perform many independent simulations. They are briefly described in the three subsections below. More details are given in the supplementary material.

The computer simulations were performed using molecular dynamics package Amber10[33] or Amber12[34] and ff03 or ff03.r1 force field,[35] appropriate for proteins. The structures of the proteins (kinesin heads and tubulins) that were used to construct the systems were downloaded from Protein Data Bank. The following structures were used: 1BG2,[36] 1MKJ[37] (both are human kinesin-1 motor domain, Kif5B), 1JFF[38] (tubulin alpha and beta chain from *Bos taurus*), 2P4N,[39] and 2XRP[40] (described in detail in the supplementary material). As in our previous studies,[29,32,41] we used SPC/E water model (extended simple point charge model).[42] Some simulations were performed with modified water models (called mod10 and mod20), as described below.

All the simulations were performed under NPT conditions (constant temperature 298 K, constant pressure 1 bar). The time step during all production runs was equal to 2 fs. A 1.2 nm cutoff for nonbonding interactions was used. Details of the simulation protocol varied between the systems, as described below and in the supplementary material.

A. Measurements of the force generated by the neck linker

For these simulations, a structure of a kinesin motor domain with a docked neck linker was used (PDB ID: 1MKJ[37]). This structure contains a bound adenosine diphosphate (ADP) molecule. A part of it was also used by Hwang *et al.*[23] in their measurements of the force. It is said that the neck linker docks to the head upon ATP binding, but Sindelar and Downing[39] pointed out that when the kinesin head is not bound to the microtubule, the linker can be in either ordered or disordered state, what is not correlated with the state of the bound nucleotide. Anyhow, since the neck linker of this kinesin motor domain is docked, we assume that there is a sufficient resemblance to the real, microtubule-bound state with a docked neck linker.

The preparation of the systems to measure the force was a multi-step procedure (described below in four steps and summarized in Fig. S4 of the supplementary material). The goal was to obtain the conditions as close to the real process of the binding of the neck linker as possible to simulate within a reasonable time.

1. Preparation of the kinesin motor domain in water

The kinesin motor domain was solvated with SPC/E water and the system was equilibrated (NPT conditions, about 1 ns; more details are given in the supplementary material).

2. The pulling of the neck linker

Three conformations (called conf_1, conf_2, and conf_3) from the equilibrated trajectory were randomly chosen, and for each one of them, the neck linker was pulled away from its binding site on the catalytic domain with the use of an external force. Three independent simulations of pulling in each direction were performed for each equilibrated conformation (these simulations were called pull_1, pull_2, and pull_3). The motivation for choosing three conformations conf_i and performing three simulations of the pulling pull_j for each one of them (instead of just one) was to make sure that our conclusions are not conformation-specific. With the available literature data, we could not *a priori* assume that our results would be conformation-dependent or conformation-independent. There was no reason to deliberately choose one conformation and reject the others. In fact, we should probably not expect that the conformation of each part of the kinesin motor (including the neck linker) is exactly the same during the same phase of

all steps it takes because of the heterogeneity of the cellular environment and the thermal motions. Therefore, to improve the reliability of our results, we analyzed more than one conformation. It turned out that the use of nine separate systems proved to be very helpful during the analysis because of the relatively high dispersion of the results—as we will discuss later.

Two directions of the pulling of the neck linker were used (called "$\alpha 7$" and "$\alpha 7 - \beta 10$") to unbind the linker and to drag it away from the catalytic domain. Both pulling directions are drawn as vectors in Fig. 1. At this stage, it gives $3 \times 3 \times 2 = 18$ systems. The choice of the directions of the pulling vectors was inspired by the article by Hwang *et al.*[23] Because of our more realistic approach (our simulation box contained a whole motor domain, not only its small part), we were unable to analyze (in a reasonable time) as many different orientations of the linker as Hwang *et al.*[23] did. The first direction ("$\alpha 7$") was approximately perpendicular to the direction appointed by the neck linker resting on the catalytic domain. The second direction ("$\alpha 7 - \beta 10$") had a significant component pointing in the direction opposite to the direction of motion of the motor. We chose these directions because the neck linker prior to the generation of the force is pointed at the opposite direction to the direction of the movement (it points to the direction of the second head—the one that later detaches from the microtubule and translates forward, past the bound head). In spite of all simplifications that were unavoidable, we wanted to use the systems that can be related to the physical reality of the movement, whenever possible.

It is known that during the working cycle of the kinesin, the docking of the neck linker occurs when the kinesin head is bound to the microtubule. Our system was a single kinesin head in water. The connection with the microtubule was modeled with a restraining force applied to selected atoms, following the idea of Hwang *et al.*[23] These restraints prevented the entire molecule from moving during the pulling.

When the neck linker detached from the head, we proceeded to the next stage—the simulations of its movement after the release from the pulling force.

3. The rebinding simulation

At first, the helix $\alpha 7$ was removed from the ends of all analyzed proteins (amino acids from 334 to the end). It was done to speed up the calculations (thanks to the reduction in the number of atoms in the systems). Each system was solvated with SPC/E water. Then, the newly added solvent was equilibrated—the protein was restrained during this period. Finally, the only restrained atoms were the ones at the bottom of the kinesin, at the tubulin binding site. The neck linker was therefore able to move freely toward its binding site (or any other way). Then, simulations were performed to measure the force generated by the cover neck bundle at increasing time from the release from the pulling force (with SPC/E water model or one of the solvents with artificially modified properties).

4. Simulations for the measurements of the force

From the rebinding trajectories, several conformations were chosen to calculate the force. The selection started from taking one conformation as a reference. Then, from each 18 trajectories, we attempted to select a conformation with an angle between the neck linker and the motor domain very similar to the reference one. Subsequently, the next conformations were chosen at specific time points after the moment when the selected start conformations occurred. They were called "2," "10," "20," "40," "60," "100," "150," "250," "350," and "650"—the time that passed from the reference moment was equal to 2 ps, 10 ps, 20 ps, and so on. The conformations "2" are presented in Fig. S5 of the supplementary material. As we can see, each time they were fairly similar, though the sheets of the cover neck bundles were always arranged a bit differently. The values of the root mean square deviation of atomic positions (RMSDs) for the CNBs and whole protein molecules can be found in the supplementary material (Tables S3 and S4). All conformations of the CNB for all stages from "2" to "650" (for two exemplary trajectories) are presented in Fig. 5.

Since our goal was to investigate the influence of the solvent, whenever it was necessary, the original SPC/E water model was substituted by the modified one (mod10

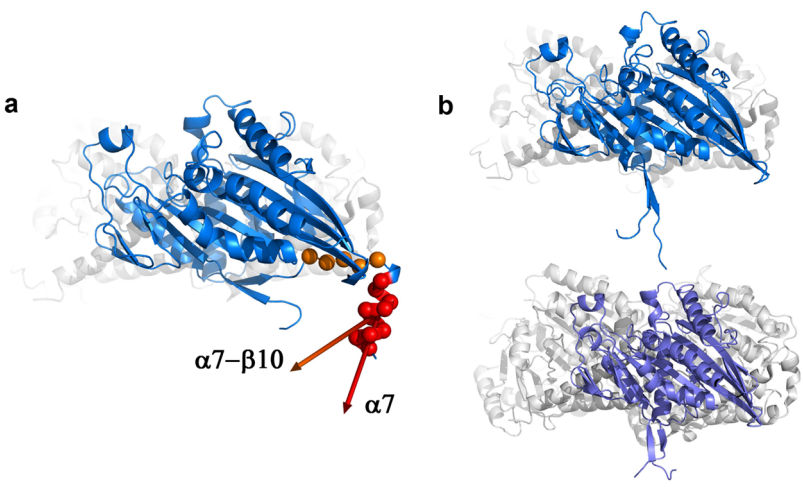

FIG. 1. (a) Pulling directions "$\alpha 7$" (the vector is parallel to the axis of the $\alpha 7$ helix) and "$\alpha 7 - \beta 10$" (the vector is a difference between the vector parallel to the axis of the $\alpha 7$ helix and the vector running through the neck linker) as vectors extending from the $\alpha 7$ helix. The atoms used to define the vectors are shown as red (339-348, $\alpha 7$ helix) and orange (332-336, the end of the neck linker) spheres. In light gray, tubulin dimer is added as a reference. (b) One example of the position of the neck linker after the pulling in "$\alpha 7$" (top) and "$\alpha 7 - \beta 10$" (bottom) directions and trimming of the terminal $\alpha 7$ helix. The structures of the proteins were drawn with PyMOL.[43]

or mod20) and the new solvents were equilibrated with the protein restrained. The modified water models helped us previously[14,32] to capture and explain several features of the behavior of the proteins; therefore, we decided to use them here again for simulations set up to measure the force. The modifications were inspired by the idea described by Sorin *et al.*[44] The Lennard-Jones potential parameters ϵ and σ of the oxygen atom of SPC/E water molecule were simultaneously altered so that the density of water remained unchanged. The geometry of water molecule and the partial charges of all atoms also remained the same. The models prepared by us according to this procedure are called mod10 (decreased ϵ, increased σ) and mod20 (increased ϵ, decreased σ). They are described in more detail in the supplementary material.

As Sorin *et al.*[44] described, by increasing the Lennard-Jones potential well depth by increasing the ϵ parameter of the oxygen atom of the molecule of water, the energetic benefit of forming close van der Waals contact between solute and solvent is increased. This way, the solute becomes less solvophobic. By decreasing the Lennard-Jones potential well depth by decreasing the ϵ parameter, the energetic benefit of forming close van der Waals contact between solute and solvent is decreased. This way, the solute becomes more solvophobic. The former applies to the mod20 model and the latter to the mod10 model. Therefore, the water models ordered according to the decreasing protein-solvent attraction energy (increasing solvophobicity) are as follows: mod20, SPC/E, mod10.

As can be found in the supplementary material (Table S1), the modified water models have different structural and dynamical features than the SPC/E model (although the density is maintained). The mod10 model has got a smaller diffusion coefficient, creates (on average) more hydrogen bonds, and the bonds have higher energy. Conversely, mod20 model has got a greater diffusion coefficient, creates (on average) less hydrogen bonds, and the bonds have smaller energy.

After the equilibration of the solvent, new simulations were performed to measure the force. They had to be conducted in a specific way. The α-carbon atom of the residue 331 (valine) had to be restrained by a harmonic potential. The force constant was $k = 10$ kcal mol^{-1} Å^{-2}, as suggested by Hwang *et al.*[23] The other restrained atoms were the ones at the bottom of the kinesin, at the tubulin binding site (as previously). The change in the model did not lead to the disruption of the structure of the proteins, as is discussed in the supplementary material.

The summed length of the analyzed trajectories (for one pulling direction, for one water model, for one conformation, for one simulation of pulling, and for one stage of docking) was equal to about 100 ns for the most numerous samples. A single result was obtained from a 0.5 ns long part of the trajectory. The number of results used to calculate the averages can be found in Figs. S12 and S13 of the supplementary material. Unfortunately, it turned out that the dispersion of the results was high. That resulted in some difficulties in the interpretation of the measured values of the force. How they were overcome is discussed below, in the Results section.

The formula to calculate the force $\vec{F}(\vec{r}_0) = [F_x, F_y, F_z]$ at some selected point $\vec{r}_0 = [r_{x0}, r_{y0}, r_{z0}]$ can be found in Hwang *et al.*,[23] along with its derivation:

$$F_i = \langle r_i - r_{i0} \rangle \frac{k_B T}{\langle (r_i - r_{i0})^2 \rangle - \langle r_i - r_{i0} \rangle^2} \qquad i = x, y, z. \quad (1)$$

The $\vec{r}_0$ symbol stands for the reference coordinates of the α-carbon atom of the residue 331 (valine), $\vec{r}$ stands for the actual coordinates of the atom, T is the temperature, and k_B is the Boltzmann constant. As it follows from this equation, to calculate the force from the trajectory of the system, we measure the displacement from the reference point. These fluctuations may be prone to local and instantaneous fluctuations of density of water, as well as to the fluctuations of the protein itself. Completely random fluctuations around the reference point would of course result in $\langle r_i - r_{i0} \rangle$ equal to zero, and hence, the force would be equal to zero. If the fluctuations occur predominately in one direction, then the vector of the force pointing in that direction can be obtained with this equation.

B. The dragging of the kinesin head along the short protofilament

To check whether it is possible to displace the kinesin head in a reasonable time by applying the force comparable with the one measured in the previous step, we constructed systems consisting of a kinesin head and a five-tubulin-long protofilament (Fig. 2), using the following structures: 1BG2,[36] 1MKJ,[37] 1JFF,[38] 2P4N,[39] and 2XRP.[40] The kinesin head that travels through the solvent to the next binding site contains ADP and its neck linker is undocked. Therefore, we used here 1BG2 structure, which is essentially the same protein as 1MKJ but with undocked neck linker. Unfortunately, the 1BG2 structure is smaller than 1MKJ—a short, helical fragment of the neck is missing. Since we wanted the kinesin to be pulled by an external force by the neck, we attached the neck from the 1MKJ structure at the end of the 1BG2 structure. The five-tubulin-long protofilament was build using the 1JFF structure (a tubulin dimer with bound guanosine triphosphate (GTP), diphosphate (GDP), and Mg^{2+} ion) and the 2XRP structure (this structure describes the structure of a microtubule and contains previously obtained structures of tubulins, 1JFF and 3HKE,[45] docked into a cryo-electron microscopy map). The 2XRP structure does not specify the conformation of so-called E-hooks. These are long, C-terminal polypeptide chains and were not localized during the experiment due to their highly flexible conformation. It is not clear what is their exact conformation during the work of the kinesin, but they are believed to contribute to the work of the kinesin and to influence the strength of interaction between the kinesin and the microtubule.[46,47] We also suspected that their presence might influence the speed of the movement of the kinesin dragged above the protofilament. Therefore, we decided to construct some systems with these sequences added and some without them. Straight polypeptide chains were added and then they were allowed to relax and equilibrate.

We expected that the speed of the kinesin could depend on the distance between the protofilament and the kinesin head. Because of this, the kinesin head was moved above the microtubule by three different distances: about 1.0, 1.5, and 2.0 nm (relatively to the microtubule-bound state, described

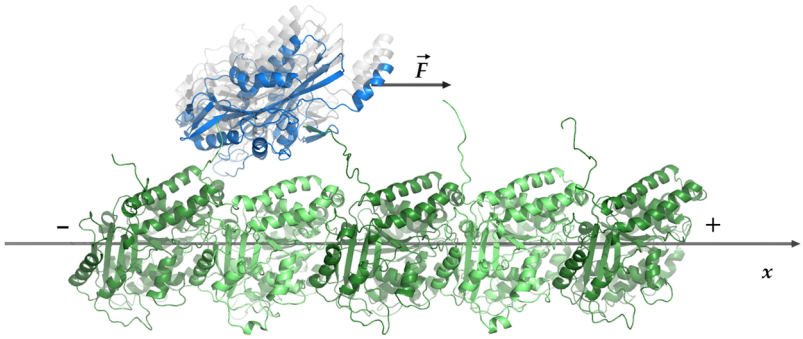

FIG. 2. The system constructed to perform the pulling of the kinesin head (in blue and light gray) along a five-tubulin-long protofilament (in green: α-tubulin in dark shade, β-tubulin in light shade). The plus and minus ends of the protofilament are indicated. The strands protruding from the tubulins are the E-hooks. The distances of the kinesin head from the protofilament were equal to approximately 1.0 (in blue), 1.5, and 2.0 nm (in light gray). The long axis of the protofilament (x) and the vector of the force applied to the neck helix ($\vec{F}$) are depicted.

by the 2P4N structure). Its position along the long axis of the protofilament was also adjusted. This is depicted in Fig. 2. The preparation of these systems is described in more detail in the supplementary material.

The forces equal to about 14, 28, 56, 112, and 224 pN were applied to the neck helix. These values were chosen to be comparable with the forces measured in the first step of the studies. Since the protofilament in a real microtubule is a part of a much bigger structure and is restrained by the presence of its neighbor protofilaments, we decided to restrain it by restraining the α-carbon atoms of the central β-sheets of the five tubulins (k = 5 kcal mol^{-1} Å^{-2}).

C. The association of the kinesin head and the tubulin dimer

To construct the systems for these simulations, we used the following structures: 1BG2,[36] 1JFF,[38] and 2P4N.[39] We analyzed the kinesin head that was initially set at four different distances from the tubulin dimer, what was supposed to represent various stages of association of the head to the binding site at the surface of the dimer. To obtain the systems for the simulations, we manually moved the kinesin from the 2P4N structure (the kinesin head bound to the tubulin dimer) above the tubulin dimer by 0.4, 0.8, 1.2, and 2.0 nm. More details about the preparation of these systems can be found in our previous article[29] and in the supplementary material. The C-ends of the tubulins were omitted as in our previous investigations of similar systems.[29,30,32] For each initial distance (0.4, 0.8, 1.2, and 2.0 nm), ten systems were prepared, with slightly different initial conformations of the kinesin head and the tubulin dimer. The overall time of the simulations differed depending on the starting distances between the kinesin and the tubulin and was equal to several dozens of nanoseconds.

III. RESULTS AND DISCUSSION

The text below is divided into three main sections, all devoted to the influence of water on the stepping of the kinesin. In Sec. III A, we demonstrate that water participates in the force-generating mechanism of the kinesin and we hypothesize what factors might contribute to this effect. Additionally, we discuss if and how the generated force changes with the stage of the docking of the neck linker. In Sec. III B, we assess the relevance of the values of the measured forces in relation to the kinetics of the stepping of the motor. In Sec. III C, we discuss the kinetics of the association of the kinesin head and the tubulins and also discuss the influence of the properties of water on this process.

A. The solvent participates in the force-generating mechanism of the kinesin

The docking of the neck linker is considered a crucial event in the working cycle of the kinesin. Our results allowed us to confirm the hypothesis that the properties of the solvent influence the process of the generation of the force, as explained below.

The statistical dispersion of the measured values of the force was found to be quite large, and the differences between the investigated water models were not always very impressive. As we suspect, the reason for this was the complexity of our systems (as mentioned in the Methods section). Hwang *et al.*[23] used only a small, isolated part of the protein and implicit solvent, while we used a whole motor domain and explicit solvent. This introduced another factor that can cause disturbances—constantly moving molecules of water that change their arrangement and collide with the protein. Because of the high dispersion of the results, we wanted to confirm that the differences in the mean values are statistically significant. We used the Welch's t-test.[48] It is more reliable for two samples with unequal variances and is also often recommended for skewed distributions[49] (the histograms of the obtained values are shown in Fig. S12 of the supplementary material). All tests were performed in R[50] (see also the supplementary material).

1. The first analyzed stage of the rebinding of the neck linker ("2")

We began with a thorough analysis of the first stage of the rebinding (the one named "2," as described in the Methods section). Many calculations were performed in order to collect numerous samples of the results, which were equal to about 200 (the exact numbers in Fig. S12 of the supplementary material) for each specific simulation out of 54: three conformations of the protein (conf$_i$, i = 1, 2, 3) pulled three times (pull$_j$, j = 1, 2, 3) in two different directions ("α7" and "α7 – β10") and immersed in three different water models (mod10, SPC/E, and mod20). The mean values of the results obtained for all of these independent simulations can be found in Fig. 3. The extent of the boxes and the whiskers in Fig. 3 illustrate the fluctuations of the measured values. The calculated standard deviations of the means are quite low, thanks to the numerous samples.

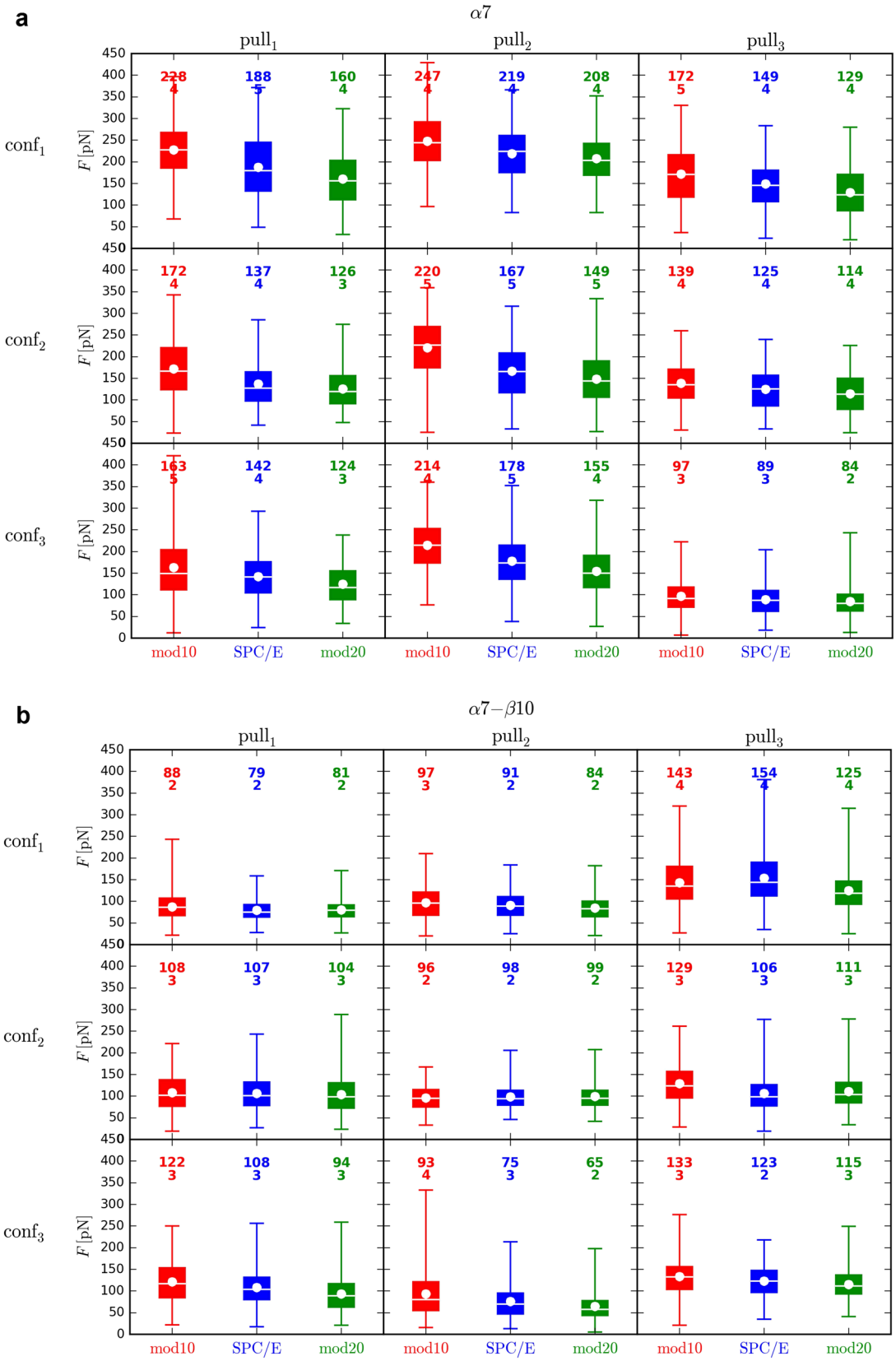

FIG. 3. The values of the force F (pN) for each water model and for the first stage of the movement of the neck linker ("2") for the "$\alpha 7$" pulling direction (a) and the "$\alpha 7 - \beta 10$" pulling direction (b). The box extends from the lower to the upper quartile values. The white horizontal line is the median. The white circles are the averages. The whiskers extend from the minimum to the maximum measured value of the force. The values above the boxes are means and standard deviations of the means, rounded to the nearest integer. All charts were drawn with Matplotlib.[51]

There are differences between the mean values of the force for different water models (Fig. 3 and Table S8 of the supplementary material). For "$\alpha 7$" pulling direction, the mean values for the SPC/E water model are always lower than for mod10 model and always higher than for mod20 model (9 out of 9). Moreover, for mod10 model, all results of the statistical tests suggested that the means are different. For mod20 model, the tests did not confirm that the means are significantly different for only two systems. The results for the "$\alpha 7 - \beta 10$" pulling direction have the same pattern most of the time (7 out of 9 means higher for mod10 and 6 out of 9 means lower for mod20). In this case, for both mod10 and mod20 models, 5 out of 9 results of the tests suggested that the means are different. What is very important is that the tests did not suggest any significant difference between the means when the mean for mod10 incidentally happened to be smaller than for SPC/E and when the mean for mod20 incidentally happened to be greater than for SPC/E (see Fig. 3 and Table S8 of the supplementary material).

There is an apparent difference between the mean values of the forces (Fig. 3) for both the pulling directions. Generally, for "$\alpha 7 - \beta 10$" pulling direction, the forces were smaller. The difference between the results for the pulling directions can be explained, as we suspect, by the different conformations of the neck linker and its surrounding forced by the different directions of the pulling vector. The cover neck bundle, as a result of pulling, became a little more bent and distorted for the "$\alpha 7 - \beta 10$" direction than for the "$\alpha 7$" direction. This points out to the significance of the cover neck bundle and its proper conformation to the effective work of the motor. For a very approximate estimation of the distortion of the cover neck bundle, notice a little higher average root mean square displacements of the core residues of the cover neck bundle from a reference conformation with a docked neck linker (Table S3 of the supplementary material) for "$\alpha 7 - \beta 10$" direction. This is accompanied by a bit higher energy of interactions between the core residues of the two strands of the cover neck bundle for "$\alpha 7$" pulling direction than for "$\alpha 7 - \beta 10$" pulling direction (Table S5 of the supplementary material). From Fig. 3, we can see that there are also some differences between the forces measured for specific conf$_i$:pull$_j$ simulations (for the results of the statistical tests, see Table S7 of the supplementary material). Within the conf$_i$:pull$_j$ systems, no exact correlation can be observed between the RMSDs of the cover neck bundles (Table S3 of the supplementary material) and the mean value of the force, what leads us to the conclusion that the value of the exerted force cannot be always and fully explained (or predicted) by calculating the RMSD of the cover neck bundle. Probably, it should be assumed that the relationship between the instantaneous structure and the force is complicated, and hence, it does not suffice to analyze only the cover neck bundle. As we mentioned in the Methods section, it can be expected that there are some random structural differences between the conformations of the protein during consecutive steps, including the conformation of the cover neck bundle. Hence, on the basis of our results, we can expect that the generated force probably is not always exactly the same in every step. However, even these smaller forces measured by us are probably enough to propel the motor forward, as we will discuss below.

2. The subsequent stages of the rebinding of the neck linker

The force was also analyzed over the trajectory of the movement of the unrestrained neck linker (the rebinding stages "2," "10," "20," and so on, as described in the Methods section). Because it would be extremely demanding time-wise to obtain for each stage as high number of results as for the first one ("2"), we collected a smaller number of results for each stage (for each conf$_i$:pull$_j$ system). One system (for each pulling direction: "$\alpha 7$" and "$\alpha 7 - \beta 10$") was chosen as a representative, with increased sampling. While making this choice, we took into account two criteria. First, we wanted the mean values of the force measured for the three water models for the representative system to be close to the overall mean value calculated for all nine systems. Second, we wanted the skewness of the distribution of the values not to be too high, if possible. This led to the choice of the conf$_1$:pull$_2$ system for "$\alpha 7$" pulling direction and conf$_3$:pull$_1$ system for "$\alpha 7 - \beta 10$" pulling direction.

We decided to present the means and the scatter of the values of the forces for all nine independent simulations conf$_i$:pull$_j$ gathered together (Fig. 4) and also means and scatter for each simulation independently (Fig. S13 of the supplementary material). Of course, it could be argued that the results conf$_i$:pull$_j$ should not be collected together, since they differ in terms of their means and the shape of their distributions. However, some differences in conformations between the systems that in our case were present at the start of the simulations may be regarded as a representation of randomness that is most probably intrinsically present in the behavior of the motor anyway. Collecting the results together was supposed to help us obtain more representative, more general, and less case-sensitive picture.

For the "$\alpha 7$" pulling direction, the values of the force apparently tend to diminish a bit with time, especially at the beginning (Fig. 4 and Fig. S13 of the supplementary material). The force is smaller for most of the stages following the stages "2" and "10." Also for stages "20" and "40," the means are higher than for the following stages. For the $\alpha 7 - \beta 10$ pulling direction, the values do not change that noticeably over time. As discussed above, we can attribute this to the differences in the degree of conformational changes in the CNB after the pulling of the neck linker. For two examples of the positions of the CNBs in consecutive stages of the docking, see Fig. 5.

Hwang *et al.*[23] also reported that the value of the force depends on the conformation of the CNB. However, as we mentioned, their methodology was different. They did not measure the forces for a real path of the rebinding of the neck linker, but they were applying a sampling potential at selected points in space, around the end of the CNB cut from the structure of a kinesin with a docked neck linker. Therefore, our results cannot be compared directly (but they are not mutually exclusive).

Moreover, Hwang *et al.*[23] found that the vectors of the force were pointing to the direction of the expected movement of the neck linker (toward its binding site), irrespectively from the initial direction of the pulling. We found a similar

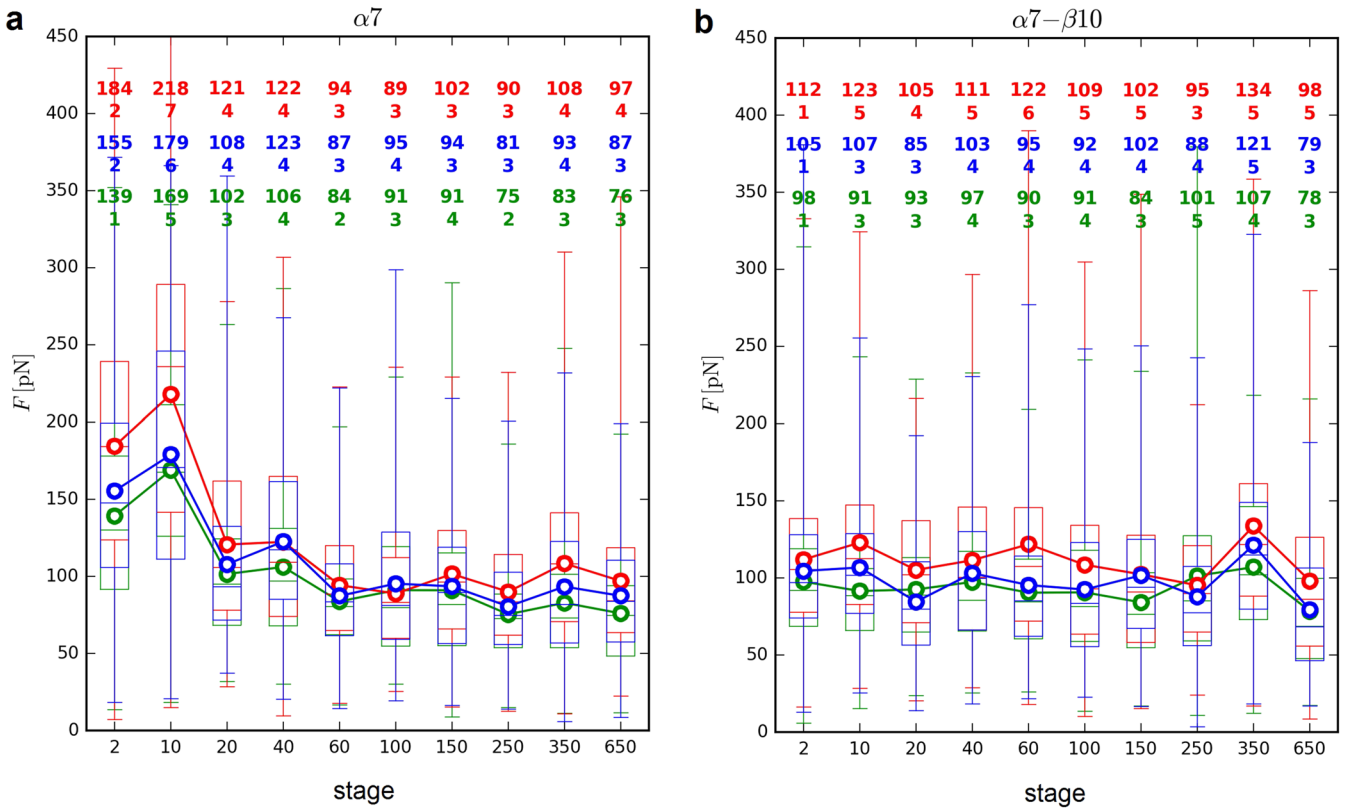

FIG. 4. The values of the force F (pN) for each water model and for each stage of the movement of the neck linker for the "$\alpha 7$" pulling direction (a) and the "$\alpha 7 - \beta 10$" pulling direction (b). The box extends from the lower to the upper quartile values. The horizontal line is the median. The whiskers extend from the minimum to the maximum measured value of the force. The white circles are the averages. The values above the boxes are means and standard deviations of the means, rounded to the nearest integer. The colors are the same as previously: red—mod10, blue—SPC/E, and green—mod 20.

tendency (Fig. 5). This was not bound to occur because a whole motor domain was taken into account, instead of a small, isolated fragment of it. We also bore in mind the results from Ref. 25, where a kinesin Ncd was described and a connection between the force vectors and the direction of motion was not found.

We were interested in the vectors of the force at preliminary steps of the neck linker docking and did not cover the full rebinding trajectory. It can be seen in Fig. 5—the neck linker (in gray) is still a bit bent compared with the fully bound conformation (in blue).

When it comes to the influence of the solvent, the obtained results for the later stages confirm the observations made for stage "2." We compared the values for different water models measured for different stages of the movement of the linker (see Fig. 4, Fig. S13 and Table S9 of the supplementary material). Again, whenever the statistical test indicated that there is a significant difference between the water models, the mean (see Fig. 4) was higher for mod10 model and lower for mod20 model than for SPC/E model—with only one exception, discussed in the caption of Table S9 of the supplementary material. Therefore, the dependency

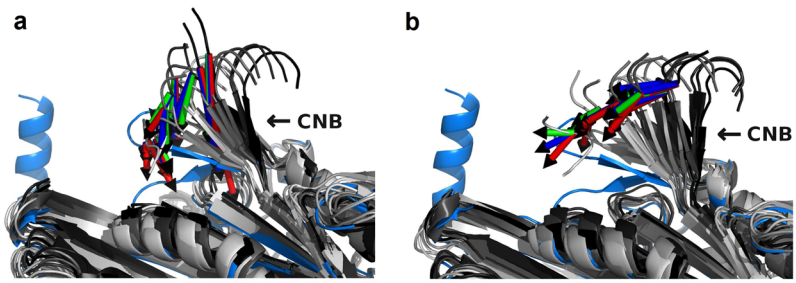

FIG. 5. Mean vectors of the force for "$\alpha 7$" pulling direction (a) and "$\alpha 7 - \beta 10$" pulling direction (b). The means are calculated over all values obtained for a given water model and stage of the docking. The water models are color-coded as follows: blue—SPC/E, red—mod10, and green—mod20. The motor domain of the kinesin is in different shades of gray: the darker one is for stage "2" and the lighter one is for stage "650." For reference, the kinesin with the docked neck linker and with the $\alpha 7$ helix is shown in blue. The arrows extend from the α-carbon atom of the residue 331 (valine). The vectors are scaled by the same factor to fit to the picture. The cover neck bundles are indicated.

of the force on the properties of the solvent is indeed present.

3. The participation of the solvent in the mechanism of the generation of the force

There may be many features of the interactions between the solvent and the protein, which could contribute to the varying force.

As it has been demonstrated, when we use the mod10 model that creates more solvophobic environment (as discussed in the Methods section), the force increases (or, sometimes, does not change by the amount that can be considered significant based on our results). When we use the mod20 model that creates less hydrophobic environment, the force decreases (or does not change).

In a recently published paper, Geng *et al.*[52] described a force required to *unbind* the neck linker from the catalytic domain (the situation opposite to the one described here). The authors describe various kinds of interactions, such as hydrogen bonds, salt bridges, water bridges, and hydrophobic interactions, between the neck linker and the head, which can influence the value of this force. We studied a different process than Geng *et al.*[52] and CNB was not fully rebound (Fig. 5). Therefore, the results of Geng *et al.*[52] cannot be directly compared with ours. The increased value of the force measured by us for the more hydrophobic conditions may support the statement of the importance of the hydrophobic interactions. Possibly, the increased solvophobicity may help in keeping the linker and the cover strand together tightly.

When we compared the mean energies of interactions of the four core residues of the CNB from one strand with the four core residues of the CNB from the second strand, we obtained slightly different results for the three water models (Table S5 of the supplementary material). The sample was not very numerous, as indicated by the caption of Table S5 of the supplementary material, but for both the pulling directions, the energy of interactions was increased for the systems with mod10 model and decreased for the systems with mod20 model—comparing with the SPC/E model (although between mod10 and SPC/E for "$\alpha 7$" pulling direction, the difference was miniscule). The energies increased in the same order for the three models as the values of the measured forces increased. Moreover, because the generation of the force should be viewed as a process that collectively engages and affects the whole domain (for example, the nucleotide binding site), the energies of Coulombic and Lennard-Jones interactions between all atoms of the protein were calculated (excluding atoms separated by three and less bonds). These results confirm that for mod10 model, the energy is higher than for SPC/E model, while for mod20 model it is lower. Therefore, the change in the solvent slightly affects the way in which the amino acids interact with each other (note that the overall shape of the protein is maintained—see the supplementary material). This leads to the modification of the values of the generated force.

This modification of the inner protein interactions should be analyzed as originating from the properties of the solvent within the solvation shell. Apparently, while all bulk water models have almost the same density, the densities of the solvation shells differ. The density of the solvation shell created by mod20 model is slightly higher than the density of the solvation shell created by SPC/E model, and both are higher than in the case of mod10 model (notice differences between radial distribution functions in Fig. S6 of the supplementary material). As we discussed previously,[64] the changes in the densities of solvation water are caused by disruption of the ordered structure of hydrogen bonds. Mod10 model creates, on average, more hydrogen bonds than SPC/E model, and the energy of these bonds is higher (Table S1 of the supplementary material). The opposite is true for mod20 model. Therefore, in the case of mod10 model, water-water interactions will be favored more than in the case of SPC/E model, and in the case of mod20 model, water-water interactions will be favored less. As a consequence, also water-protein interactions will be affected (higher density of solvation water means higher energy of interactions between the protein and its solvent).

The modification of the interactions of atoms within the cover neck bundle may affect the rigidity of this structural element, and the stiffness is crucial for the force generation, according to the existing models. Additionally, we analyzed the stiffness of the solvation water. When we compare the power spectra of the translational velocity autocorrelation function of water in the solvation layers (Fig. S6 of the supplementary material), we notice that the first, highest peak is shifted in two opposite directions for mod10 and mod20 models (comparing with the original position of SPC/E model). The first peak is commonly associated with the rigidity of the structure of water (a molecule moves in a cage created by its neighbors).[29,53–55] The shift to higher frequencies (mod10 model) can be interpreted as an increased rigidity of the structure of water and the shift to lower frequencies can be interpreted as a decreased rigidity (mod20 model).

These hypothesized mechanisms of influence of the solvent on the measured force are not, of course, mutually excluding. Moreover, it is possible that there are many more factors contributing to the effect, beside from the ones mentioned above. Overall, the interplay between the solvent and the solute is a complicated and multithreaded problem. Because of this, the exact mechanism of the participation of the solvent in the force-generation process is extremely difficult to describe.

B. The order of magnitude of the force generated by the neck linker is the same as the order of magnitude of the force that is needed to effectively pull the kinesin head along the microtubule protofilament

The distance that the kinesin head has to travel along the microtubule from the site of detachment to the site of binding during a single 8-nm-long step of the whole motor is equal to about 16 nm.[2,56] The speed of the kinesin may reach about 800 nm/s, although the time of a single step is as short as about 20 μs because of the waiting time between steps.[16,17,27,57] However, the speed of the moving head is not uniform throughout the whole trajectory of the movement. Zhang and Thirumalai,[16] using coarse-grained simulations, distinguished three major stages in the kinematics of the step.

The first one is the neck linker docking accompanied by a relatively robust displacement of the trailing head for about 5 or 6 nm. The second stage is an anisotropic translational diffusion, which moves the head for additional 6–8 nm. The last stage, during which the head travels for about 3–4 nm, is the completion of the step and binding to the binding site.

Recently, Mickolajczyk *et al.*[58] and Isojima *et al.*[59] experimentally visualized processive movement of the kinesin. They tracked the movement of an individual motor domain during the full walking cycle, including the binding and unbinding of the kinesin head to and from microtubule. They observed diagonal displacements of the unbound head, with highly diffusive movement in between.

If we want to compare our velocity of the kinesin head dragged along the microtubule under different forces, we certainly should not compare it with the average velocity of the motor, neither with the velocity of a single step. We should analyze the kinetics of this stage of the movement that occurs during the docking of the neck linker in the bound head. Such detailed data may be difficult to obtain experimentally. Although the results of coarse-grained simulations, like the ones performed by Zhang and Thirumalai,[16] may be considered not realistic enough, we turn to them because of the lack of a better alternative. As it follows from the results of Zhang and Thirumalai,[16] the movement of the head during the docking is faster than during other stages of the step. The exact velocity is difficult to determine. Zhang and Thirumalai obtained different results depending on the details of the parameterization of their model. In one of their sample trajectories, when they used parameterization that ensured qualitative agreement with the experimental data, the displacement of the head along the microtubule axis during the docking was 5.2 nm. The time of the docking in this case was about 0.15 μs, as we learn from the supplementary material. This gives the velocity exceeding 0.03 nm/ns. As we can estimate from the data in Fig. 6, the velocity of the kinesin under the influence of

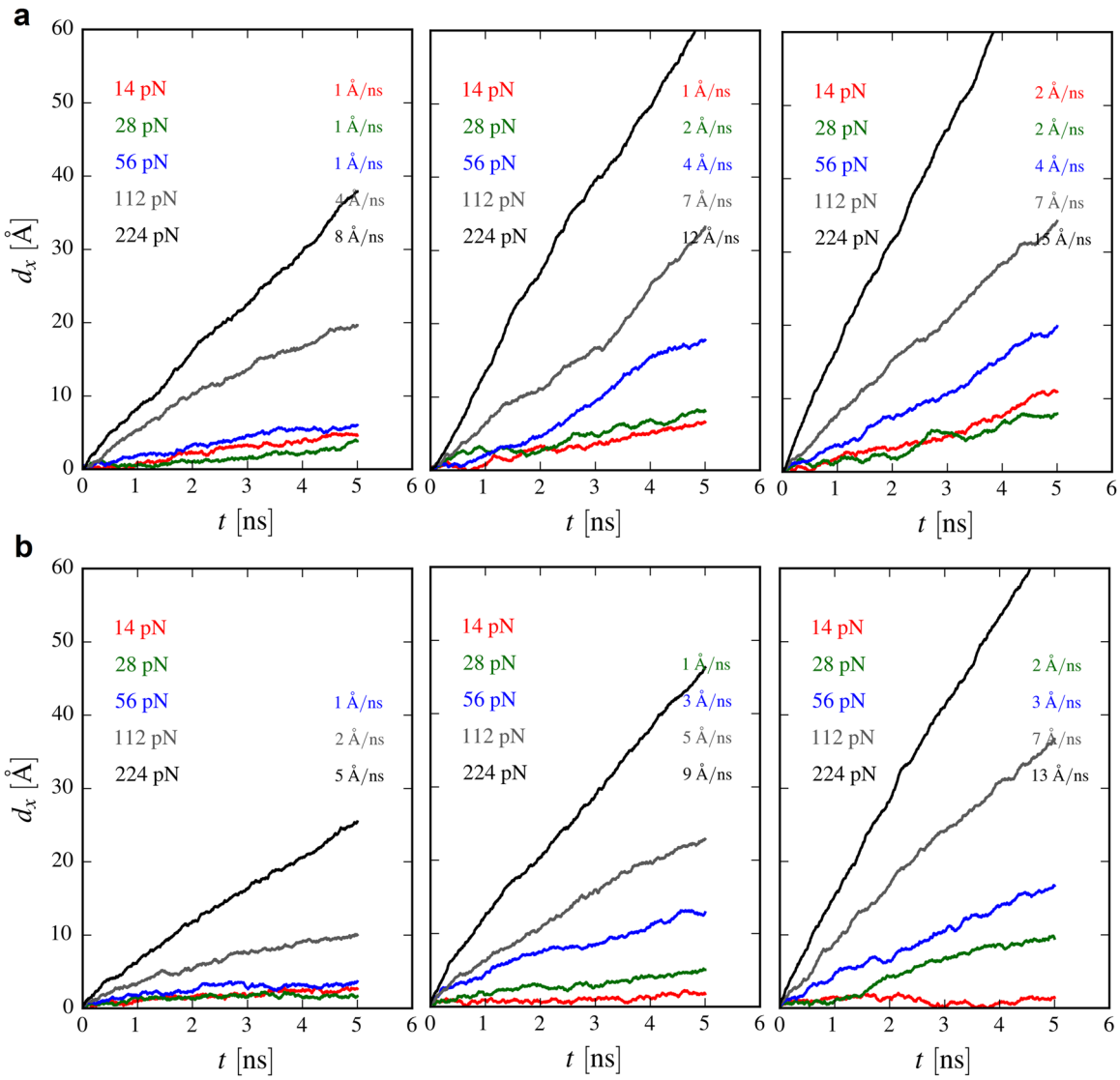

FIG. 6. The displacement of the center of mass of the kinesin head along the long axis of the five-tubulin-long protofilament (x-axis in Fig. 2) caused by the pulling of the neck helix with forces equal to about 14, 28, 56, 112, 224 pN. (a) Tubulins without the E-hooks. (b) Tubulins with the E-hooks. Results for three distances of the kinesin head to the tubulins are compared: for 1.0, 1.5, and 2.0 nm (from left to right). The results are averages from six trajectories. The velocities estimated as the ratios of the mean displacements at the end of the simulations to the simulation time are added (rounded to the nearest integer).

the force appears to be greater than that value, certainly for the forces such as 56 pN or 112 pN which correspond to the values of the generated forces measured by us. When it comes to the comparison of our estimation of the velocity with the one from the article of Zhang and Thirumalai,[16] a couple of explanations of the velocity exceeding the literature data may be possible: (1) Differences in the studied models and methodology of the measurements may lead to different results. (2) Our system is (still) not realistic enough. (3) The actual trajectory of the head during the stepping is more complex than in our study. (4) The actual force generated by the cover neck bundle may be lower than our results indicate. We also have to mention that there is a possibility that the force can change with time and, supposedly, at some stages of the docking might be significantly smaller, what was not captured by us.

The velocity depends not only on the force applied to the neck helix but also on the distance of the head from the protofilament. It is not surprising, since that process should depend on the friction of the solvent and the friction increases as we get closer to the protofilament because of the changes in the properties of the solvation water.

Friction influences the performance of biological nanomachines to a significant extent, kinesin included. Bormuth *et al.*[60] performed an experiment, during which they moved kinesin relatively to microtubule track and observed that motor-microtubule friction force depended on speed. At smaller velocities, protein friction force increased linearly with speed, but at higher velocities this relation became nonlinear. Moreover, frictional forces at higher velocities were significantly lower when the motor was dragged toward the plus end of the microtubule compared with the minus end. The forces that limit the speed of the kinesin originate, according to the authors, from the adhesive bonds between the kinesin and the binding sites on the track.[61] Our kinesin was lifted above the microtubule. Therefore, our results cannot be directly compared.

The smaller velocity in the presence of the E-hooks is clearly observed (Fig. 6), as expected, though the difference is usually not very dramatic. Bormuth *et al.*[61] also investigated the influence of the presence and absence of the E-hooks and they reported that they did not observe great differences in the results obtained for these two systems. Naturally, it does not mean that the E-hooks are irrelevant for the movement of kinesins. We also should mention that our measurements of the velocities of the head in the presence of the tubulins with the E-hooks may not reflect the behavior of the real system to the last detail, because the exact conformation of the E-hooks during each stage of the step is unknown, as far as we know.

Of course, besides the pulling force, there may be additional factors, such as electrostatic interactions, influencing the process of the movement along the protofilament. However, judging from the slopes of the obtained displacements of the head, if the electrostatic interactions contribute to the movement, they probably do not promote very fast movement—contrary to the pulling.

Our results agree with the hypothesis that the movement of the kinesin head approaching the next binding site on the microtubule is assisted by the process of the docking of the neck linker, what may be followed by a diffusional search.

C. The behavior of the proteins during the process of the association of the kinesin and the tubulin is influenced by the properties of the solvent

The systems selected for our studies consisted of a kinesin head and a tubulin dimer. We considered four different initial distances between them, equal to about 0.4 nm, 0.8 nm, 1.2 nm, and 2.0 nm. The analyzed distances represent typical distances between macromolecules in a crowded environment inside a living cell.[62]

In the case of hydrophilic association, water density between the associating proteins can be a little bit greater.[7,29] Therefore, the role of water would be rather to facilitate mutual fitting of two binding surfaces and not to accelerate the encounter by creating an empty space,[8] as may be the case for the hydrophobic collapse.

Solvation water between the kinesin and the tubulins is not only denser but also less mobile and more rigid.[29] The diffusion coefficient of the solute depends, of course, on the properties of the solvent. It appears that the interfacial water allows the proteins to approach each other relatively quickly when they are far away but can slow down the process when the proteins are closer to each other. As it can be seen in Fig. 7, the highest velocity of the approach of the head is observed for the longest distances between the associating proteins (the diffusion coefficient of the interfacial water is very significantly diminished for the shortest distance[29]).

The attempt to compare these velocities with the experiment would be difficult. We have to remember that to complete the step and to bind to the next binding site, kinesin-1 has to stretch the linker.[1,63] It might be suspected that this necessity can, to some extent, hinder the velocity of the binding to the next site. The kinesin head in our simulation did not have to move against any strain.

Ahmad *et al.*[7] demonstrated that two hydrophilic planes of associating proteins are connected with many chains of hydrogen bonds that run through the interfacial solvation water. To check how the water-mediated connection between the proteins changes in time, we resorted to graph theory and maximum flow problem, following the idea of Ahmad *et al.*,[7] used by us previously[32] to hypothesize on the role of the properties of the solvent in the partial correlation of movement of the surface atoms of the proteins. Here, we would like to check how this method can illustrate the changing properties of solvation water between the proteins when they are brought closer to each other. The goal of solving the maximum flow problem is to find the maximum flow between a source and a sink, which occurs through "pipes" represented as edges of the graph. Each edge and each vertex can have its own unique capacity. As we described in the supplementary material to Ref. 32, our approach was slightly different from the one described by Ahmad *et al.*[7] since we took into account water molecules in the first solvation shells of both analyzed protein surfaces (defined as those molecules that are

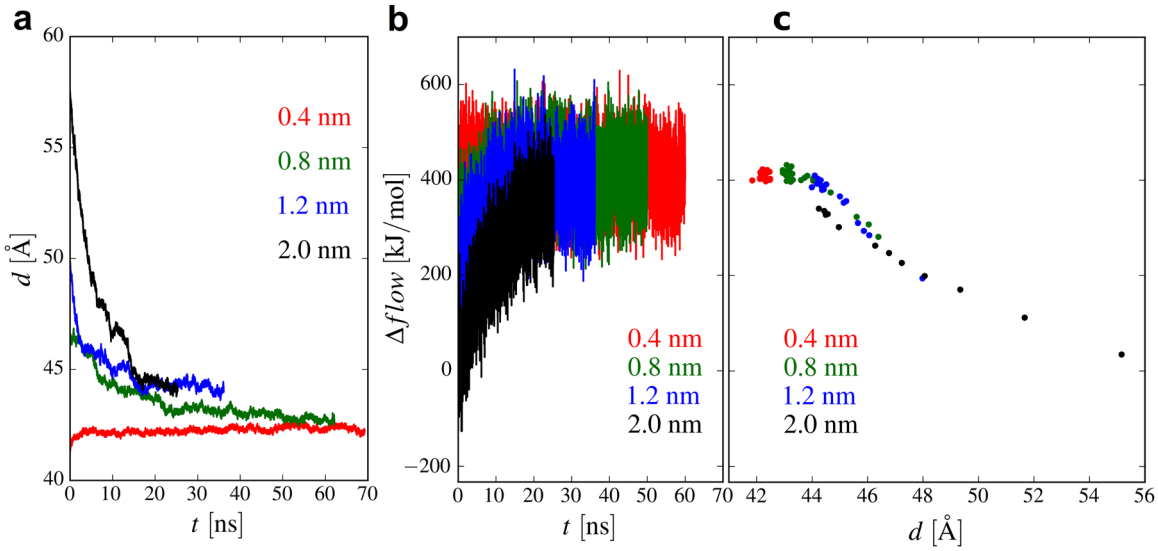

FIG. 7. (a) The distance of the center of mass of the kinesin head from the axis connecting the center of mass of the two tubulins (measured along the z-axis in Fig. S10 of the supplementary material) for simulations starting from distances 0.4, 0.8, 1.2, and 2.0 nm between the head and the tubulin. The results are averages from ten trajectories. (b) The difference in the maximum flow calculated for water present between the kinesin head and the tubulin dimer, at different stages of their association for simulations starting from distances 0.4, 0.8, 1.2, and 2.0 nm between the head and the tubulin (solvation water minus bulk water, as described in the text). The results are averages from ten trajectories. (c) The mean value of $\Delta flow$ versus the mean distance from (a), calculated within the same consecutive time spans (2 ns long). Standard deviations of the means were equal to about 5 kJ/mol.

present not farther than 0.4 nm from the surfaces of the proteins) and calculated the flow between a source connected with the molecules belonging to the solvation shell of the tubulin dimer and a sink connected with the molecules belonging to the solvation shell of the kinesin head. The edges connecting the water molecules with the source and with the sink all had the same capacity, equal to the mean energy of a hydrogen bond of SPC/E water model. The capacities of the rest of the edges, representing hydrogen bonds, were equal to the energies of the bonds. The absolute values of the flow are almost meaningless on their own. They depend strongly on the specific procedure used to determine them. Therefore, we decided to modify the procedure further and implement the idea used by us previously.[14,64] The idea was to perform reference calculations for fictitious solvation shell, filled with water whose structure is the same as the structure of bulk water. This way, when we calculate the difference between the results for the real solvation shell and the reference shell, we account for the fact that the flow depends on the distance between the source and the sink and we obtain a value that characterizes the changes in the structure of the network of hydrogen bonds. Of course, this approach is, unfortunately, also not free from drawbacks, because when the proteins are close to each other, their solvation shells partially or completely overlap, so we have to bear that in mind during the interpretation of the results.

Examining Fig. 7, we can see that the kinesin and the tubulins are connected by the tight network of hydrogen bonds that become more extensive during the process of association. It can be related to our previous results, indicating that the number of hydrogen bonds between water molecules in solvation shells can be greater (after we account for the excluded volume occupied by the protein).[14] Also, hydrogen bonds tend to become, on average, a little shorter.[29] Clearly, the slowing down of the kinetics of the association of the kinesin and the tubulins (Fig. 7) is correlated with the tightening of the hydrogen-bonded network of the interfacial water molecules. The stiffened structure of solvation water makes these water molecules increasingly difficult to remove from the space between the proteins. For the shortest distances, there are also additional factors present, which influence the kinetics, such as relative orientation of the proteins and their mutual adjustment.

IV. CONCLUSIONS

The performance of the kinesin molecular motor can be affected by the properties of the solvent. We investigated their influence on the crucial event in the working cycle, which is the docking of the neck linker (along with the movement of the head through the solvent under the influence of the force) and on the approach of the kinesin to the binding site on microtubule. The obtained results allow us to conclude that the force generated by the neck linker of the kinesin depends on the properties of the solvent. The force tends to be greater if we use the model with smaller diffusion coefficient that creates more hydrogen bonds and makes the solute-solvent interface more hydrophobic (mod10 model). On the other hand, the force tends to be smaller if we use the model with higher diffusion coefficient that creates less hydrogen bonds and makes the solute-solvent interface more hydrophilic (mod20 model). It highlights the importance of water for the process and indicates that the solvent participates in the force generation. This fact has been so far overlooked when discussing the work of the motor. The proposed explanations of the influence of the properties of the solvent on the force include the influence on the inner protein interactions, which is higher in mod10 model and lower in mod20 model. This is connected with differences

in water-protein interactions and differences in the structure and rigidity of the solvation shells created by the three water models. The modification of the inner protein interactions may affect the rigidity of the structure, considered as important for the generation of the force according to the existing models. The complex nature of interactions between water and proteins makes the investigations of the role of the solvent a complicated matter, yet worth more work in the future—it is relevant not only to the work of kinesin but also to proteins in general.

As we also observed, the force is sensitive to the actual conformation of the cover neck bundle. Different directions in which the bound cover neck bundle was pulled away from its binding site led to different deformations of the protein (especially the cover neck bundle and its surrounding). The deformation determines the pathway of the relaxation of the strain. This is probably the cause of the approximate dependence of the force on the stage of the docking for "$\alpha 7$" pulling direction and lack of the dependence for "$\alpha 7 - \beta 10$" pulling direction.

Overall, our results agree with the hypothesis that the kinesin head approaching the binding site on the microtubule might be directed by the docking of the neck linker. However, there are some subtleties that call for attention. Initially, the linker is oriented in the opposite direction than the direction of the movement of the moving head. It means that it is significantly bent from its reference docked state. As our results suggest, to generate the highest force, the cover neck bundle must fulfill strict conformational requirements. However, even the smaller forces measured by us were sufficient to effectively pull the kinesin over a short protofilament. When the discussion of the mechanics of the proteins is concerned, it is not always remembered that proteins are subject to thermal motions, constantly fluctuate, and change their structure (slightly or substantially). Our results suggest that the generated force is probably not strictly the same in every step of the motor. They also demonstrate that there is some conformational flexibility allowed to the motor without losing the desired mechanical properties and without affecting the overall performance.

When it comes to the association of the kinesin head and the tubulin, it follows from our results that the kinetics of the association of the kinesin head to the binding site at the surface of the microtubule also seems to be connected with the properties of the solvent between the kinesin and the tubulin. Initially, the approach of the kinesin to the tubulin is quite fast. Later, it slows down, which is correlated with tightening of the hydrogen-bonded net of water molecules in the interfacial region between the proteins. The stiffened structure of solvation water makes these water molecules increasingly difficult to remove from the space between the proteins.

The properties of water in living cells may change over time and may vary in different parts of the cell. The working cycle of the kinesin could be influenced by these changes in the properties of water. They could affect the force generated by the linker, the kinetics of the process of attachment of the kinesin head and the microtubule, as well as the inner conformational changes.

SUPPLEMENTARY MATERIAL

See supplementary material for the details on: the preparation of the systems and computer simulations; the results of the measurements of the force, including histograms and box-and-whisker plots of independent series of calculations; the selected properties of solvation water; and the energies of the inner protein interactions.

ACKNOWLEDGMENTS

This work was supported by the Polish National Science Centre within the research Grant No. DEC-2013/09/D/NZ1/01087. The calculations were carried out at the Academic Computer Center (TASK) in Gdańsk. This research was supported in part by PL-Grid Infrastructure.

[1] W. O. Hancock, Biophys. J. **110**, 1216 (2016).
[2] A. Yildiz, M. Tomishige, R. D. Vale, and P. R. Selvin, Science **303**, 676 (2004).
[3] F. J. Kull and S. A. Endow, J. Cell Sci. **115**, 15 (2002).
[4] B. J. Grant, D. M. Gheorghe, W. Zheng, M. Alonso, G. Huber, M. Dlugosz, J. A. McCammon, and R. A. Cross, PLoS Biol. **9**, e1001207 (2011).
[5] L. Li, J. Alper, and E. Alexov, Sci. Rep. **6**, 23249 (2016).
[6] Y. Levy and J. N. Onuchic, Annu. Rev. Biophys. Biomol. Struct. **35**, 389 (2006).
[7] M. Ahmad, W. Gu, T. Geyer, and V. Helms, Nat. Commun. **2**, 261 (2011).
[8] S. H. Chong and S. Ham, Proc. Natl. Acad. Sci. U. S. A. **109**, 7636 (2012).
[9] P. Liu, X. Huang, R. Zhou, and B. J. Berne, Nature **437**, 159 (2005).
[10] P. W. Fenimore, H. Frauenfelder, B. H. McMahon, and R. D. Young, Proc. Natl. Acad. Sci. U. S. A. **101**, 14408 (2004).
[11] A. L. Tournier, V. Réat, R. Dunn, R. Daniel, J. C. Smith, and J. Finney, Phys. Chem. Chem. Phys. **7**, 1388 (2005).
[12] V. Helms, ChemPhysChem **8**, 23 (2007).
[13] P. Ball, Chem. Rev. **108**, 74 (2008).
[14] A. Kuffel and J. Zielkiewicz, Phys. Chem. Chem. Phys. **14**, 5561 (2012).
[15] X. Daura, A. E. Mark, and W. F. van Gunsteren, Comput. Phys. Commun. **123**, 97 (1999).
[16] Z. Zhang and D. Thirumalai, Structure **20**, 628 (2012).
[17] Y. Goldtzvik, Z. Zhang, and D. Thirumalai, J. Phys. Chem. B **120**, 2071 (2015).
[18] B. E. Clancy, W. M. Behnke-Parks, J. O. Andreasson, S. S. Rosenfeld, and S. M. Block, Nat. Struct. Mol. Biol. **18**, 1020 (2011).
[19] F. J. Kull and S. A. Endow, J. Cell Sci. **126**, 9 (2013).
[20] S. Rice, A. W. Lin, D. Safer, C. L. Hart, N. Naber, B. O. Carragher, S. M. Cain, E. Pechatnikova, E. M. Wilson-Kubalek, M. Whittaker, E. Pate, R. Cooke, E. W. Taylor, R. A. Milligan, and R. D. Vale, Nature **402**, 778 (1999).
[21] S. M. Block, Biophys. J. **92**, 2986 (2007).
[22] S. Rice, Y. Cui, C. Sindelar, N. Naber, M. Matuska, R. Vale, and R. Cooke, Biophys. J. **84**, 1844 (2003).
[23] W. Hwang, M. J. Lang, and M. Karplus, Structure **16**, 62 (2008).
[24] W. R. Hesse, M. Steiner, M. L. Wohlever, R. D. Kamm, W. Hwang, and M. J. Lang, Biophys. J. **104**, 1969 (2013).
[25] S. K. Lakkaraju and W. Hwang, Biophys. J. **101**, 1105 (2011).
[26] H. Yan-Bin, P. Zhang, Z. Hui, A. Li, K. De-Xin, and J. Qing, Chin. Phys. Lett. **26**, 078701 (2009).
[27] N. J. Carter and R. A. Cross, Nature **435**, 308 (2005).
[28] D. L. Ermak and J. A. McCammon, J. Chem. Phys. **69**, 1352 (1978).
[29] A. Kuffel and J. Zielkiewicz, Phys. Chem. Chem. Phys. **15**, 4527 (2013).
[30] A. Kuffel, Phys. Chem. Chem. Phys. **19**, 5441 (2017).
[31] I. Bahar, T. R. Lezon, A. Bakan, and I. H. Shrivastava, Chem. Rev. **110**, 1463 (2010).
[32] A. Kuffel and J. Zielkiewicz, Phys. Chem. Chem. Phys. **17**, 6728 (2015).
[33] D. A. Case, T. A. Darden, T. E. Cheatham III, C. L. Simmerling, J. Wang, R. E. Duke, R. Luo, M. Crowley, R. C. Walker, W. Zhang, K. M. Merz, B. Wang, S. Hayik, A. Roitberg, G. Seabra, I. Kolossváry, K. F. Wong, F. Paesani, J. Vanicek, X. Wu, S. R. Brozell, T. Steinbrecher, H. Gohlke, L. Yang, C. Tan, J. Mongan, V. Hornak, G. Cui, D. H. Mathews, M. G. Seetin, C. Sagui, V. Babin, and P. A. Kollman, *AMBER 10* (University of California, San Francisco, 2008).

[34]D. A. Case, T. A. Darden, T. E. Cheatham III, C. L. Simmerling, J. Wang, R. E. Duke, R. Luo, R. C. Walker, W. Zhang, K. M. Merz, B. Roberts, S. Hayik, A. Roitberg, G. Seabra, J. Swails, A. W. Götz, I. Kolossváry, K. F. Wong, F. Paesani, J. Vanicek, R. M. Wolf, J. Liu, X. Wu, S. R. Brozell, T. Steinbrecher, H. Gohlke, Q. Cai, X. Ye, J. Wang, M.-J. Hsieh, G. Cui, D. R. Roe, D. H. Mathews, M. G. Seetin, R. Salomon-Ferrer, C. Sagui, V. Babin, T. Luchko, S. Gusarov, A. Kovalenko, and P. A. Kollman, *AMBER 12. Reference Manual* (University of California, San Francisco, 2012).
[35]Y. Duan, C. Wu, S. Chowdhury, M. C. Lee, G. M. Xiong, W. Zhang, R. Yang, P. Cieplak, R. Luo, T. Lee, J. Caldwell, J. M. Wang, and P. Kollman, J. Comput. Chem. **24**, 1999 (2003).
[36]F. J. Kull, E. P. Sablin, R. Lau, R. J. Fletterick, and R. D. Vale, Nature **380**, 550 (1996).
[37]C. V. Sindelar, M. J. Budny, S. Rice, N. Naber, R. Fletterick, and R. Cooke, Nat. Struct. Biol. **9**, 844 (2002).
[38]J. Löwe, H. Li, K. H. Downing, and E. Nogales, J. Mol. Biol. **313**, 1045 (2001).
[39]C. V. Sindelar and K. H. Downing, J. Cell Biol. **177**, 377 (2007).
[40]F. J. Fourniol, C. V. Sindelar, B. Amigues, D. K. Clare, G. Thomas, M. Perderiset, F. Francis, A. Houdusse, and C. A. Moores, J. Cell Biol. **191**, 463 (2010).
[41]A. Kuffel and J. Zielkiewicz, Phys. Chem. Chem. Phys. **18**, 4881 (2016).
[42]H. J. C. Berendsen, J. R. Grigera, and T. P. Straatsma, J. Phys. Chem. **91**, 6269 (1987).
[43]Schrödinger, LLC, The PyMOL molecular graphics system, version 1.8.
[44]E. J. Sorin, Y. M. Rhee, M. R. Shirts, and V. S. Pande, J. Mol. Biol. **356**, 248 (2006).
[45]A. Dorleans, B. Gigant, R. B. G. Ravelli, P. Mailliet, V. Mikol, and M. Knossow, Proc. Natl. Acad. Sci. U. S. A. **106**, 13775 (2009).
[46]S. Lakämper and E. Meyhöfer, Biophys. J. **89**, 3223 (2005).
[47]S. Lakämper and E. Meyhöfer, J. Muscle Res. Cell Motil. **27**, 161 (2006).
[48]B. L. Welch, Biometrika **34**, 28 (1947).
[49]M. W. Fagerland and L. Sandvik, Contemp. Clin. Trials **30**, 490 (2009).
[50]R Core Team, *R: A Language and Environment for Statistical Computing* (R Foundation for Statistical Computing, Vienna, Austria, 2016).
[51]J. D. Hunter, Comput. Sci. Eng. **9**, 90 (2007).
[52]Y. Z. Geng, T. Li, Q. Ji, and S. Yan, Cell. Mol. Bioeng. **7**, 99 (2014).
[53]M. Cho, G. R. Fleming, S. Saito, I. Ohmine, and R. M. Stratt, J. Chem. Phys. **100**, 6672 (1994).
[54]A. Idrissi, F. Sokolić, and A. Perera, J. Chem. Phys. **112**, 9479 (2000).
[55]A. Idrissi and P. Damay, J. Non-Cryst. Solids **352**, 4486 (2006).
[56]A. B. Kolomeisky and M. E. Fisher, Annu. Rev. Phys. Chem. **58**, 675 (2007).
[57]A. Yildiz and P. R. Selvin, Trends Cell Biol. **15**, 112 (2005).
[58]K. J. Mickolajczyk, N. C. Deffenbaugh, J. O. Arroyo, J. Andrecka, P. Kukura, and W. O. Hancock, Proc. Natl. Acad. Sci. U. S. A. **112**, E7186 (2015).
[59]H. Isojima, R. Iino, Y. Niitani, H. Noji, and M. Tomishige, Nat. Chem. Biol. **12**, 290 (2016).
[60]V. Bormuth, V. Varga, J. Howard, and E. Schäffer, Science **325**, 870 (2009).
[61]V. Bormuth, V. Varga, J. Howard, and E. Schäffer, Proc. SPIE **7762**, 776208 (2010).
[62]P. Ball, ChemPhysChem **9**, 2677 (2008).
[63]C. Hyeon and J. N. Onuchic, Proc. Natl. Acad. Sci. U. S. A. **104**, 2175 (2007).
[64]A. Kuffel and J. Zielkiewicz, J. Phys. Chem. B **116**, 12113 (2012).